PROCEEDINGS OF SPIE

SPIEDigitalLibrary.org/conference-proceedings-of-spie

Impact of laser texturing parameters and processing environment in the anti-wetting transition of nanosecond laser generated textures

Godoy Vilar, J. P., Góra, W., See, T. L., Hand, D.

J. P. Godoy Vilar, W. S. Góra, T. L. See, D. P. Hand, "Impact of laser texturing parameters and processing environment in the anti-wetting transition of nanosecond laser generated textures," Proc. SPIE 11268, Laser-based Micro- and Nanoprocessing XIV, 1126818 (2 March 2020); doi: 10.1117/12.2544908

SPIE.

Event: SPIE LASE, 2020, San Francisco, California, United States

Impact of laser texturing parameters and processing environment in the anti-wetting transition of nanosecond laser generated textures.

J.P. Godoy Vilar [1,2], W.S. Gora[2], T.L.See[1], D.P.Hand[2]
[1] The Manufacturing Technology Centre, Ansty Business Park, Coventry, United Kingdom, CV7 9JU;
[2] Institute of Photonics & Quantum Sciences, School of Engineering & Physical Sciences, Heriot-Watt University, Edinburgh EH14 4AS,

ABSTRACT

Anti-wetting, or superhydrophobic surfaces have been a subject of significant interest in the engineering field for many years, particularly due to the potential to create self-cleaning surfaces. A droplet of water landing on a super-hydrophobic surface will roll or slide away, whilst taking with it any surface debris. Such surfaces exist in nature, and there have been many reports where ultra-short pulsed lasers have been used to generate surfaces with similar feature sizes and hydrophobic performance. However it is also possible to produce superhydrophobic surfaces with short (nanosecond) laser pulses.

In this paper we report our work in which flat sheets of SS304S15 were textured using a nanosecond pulsed fibre laser operating at 1064 nm. Quantitative analysis of the wettability of the laser structured surfaces was carried out by measuring the static contact angle of a droplet of deionized water with a volume in the microliter range. As with other reports, these surfaces are initially hydrophilic, and after a time delay of some days to weeks transition to hydrophobic, and in some cases to superhydrophobic. In order to realise a practical process, our work has concentrated in speeding up this transition from weeks to days, and to this end we have studied the role of the processing environment during laser texturing.

Keywords: Laser texturing, Tribology, Superhydrophobic, Short pulsed laser.

1. INTRODUCTION

Superhydrophobic structures have received increased attention in recent years due to their possible industrial applications, which include anti-icing surfaces [1] and self-cleaning surfaces [2]. These properties can also be found in nature, an example of this is the lotus leaf; in which the combination of the leaf's epicuticular wax crystals and microstructures provides anti-wetting properties [3]. Arrays of thin pillars, or hierarchical structures with roughness at two length scales have been suggesting as ways of generating superhydrophobic structures.

Laser texturing can generate patterns of varying geometries and sizes. The majority of publications that report laser texturing for generating superhydrophobic surfaces use ultrashort pulsed lasers [4], however nanosecond pulsed lasers can also be used [5]. Such laser-generated structures (whether created with nanosecond pulsed or ultrashort pulsed lasers) are initially superhydrophilic and after some time transition to hydrophobic, or in some cases superhydrophobic. The distinction between hydrophobic and superhydrophobic is in the observed dynamic behaviour of the liquid. In the hydrophobic case, water forms into droplets rather than a film, however these droplets still adhere to the surface, whereas with superhydrophobic surfaces the droplets easily roll off [5]. The final anti-wetting capabilities of the textures and the transition time are affected by the material [6], the laser processing parameters [7] and the post-processing regime [8,9].

Two possible sets of mechanisms for inducing the anti-wetting transition have been suggested in the literature. The first mechanism proposed is the hydroxylation of metal oxides generated through laser processing due to the water molecules in air. These surface hydroxyls then promote the chemisorption of organic molecules such as hydrocarbons, increasing the hydrophobicity of the surface[10]. The second mechanism proposed is related to the deposition of carbon into the surface due to the presence of non-stoichiometric active magnetite[11].

Laser-based Micro- and Nanoprocessing XIV, edited by Udo Klotzbach, Akira Watanabe, Rainer Kling, Proc. of SPIE Vol. 11268, 1126818 · © 2020 SPIE
CCC code: 0277-786X/20/$21 · doi: 10.1117/12.2544908

Many post-processing methods—aiming to accelerate the anti-wetting transition—have been reported in the literature, including storing laser textured samples in a high vacuum environment[10] or a post laser processing low annealing treatment, were samples are heat treated for several hours[12]. Our work focuses on the impact of different laser parameters as well as the role of the processing environment during laser texturing in the anti-wetting transition.

2. EXPERIMENTAL METHOD

The material used in this work is stainless steel (SS304S15) in the form of laser cut 45 mm × 45 mm flat coupons of 1 mm thickness. The laser texturing was carried out using a GF AgieCharmilles LASER P400U, a 5-axis system with an integrated nanosecond laser (IPG YLPN 30W) operating in the infrared (wavelength 1064 nm). The laser beam is delivered onto the material using a scanning galvanometer and a 160 mm f-theta lens with a nominal beam diameter at focus of 50 µm. This system is capable of texturing complex geometries; however, for this work texturing was carried out only in a flat plane. The laser was operated at a repetition rate of 25 kHz and pulse duration of 200 ns. The textures were generated using two passes, as shown in Figure 1, where the second pass is perpendicular to the first, and the scanning direction alternates. Samples were processed with varying scan line separation—from 25 µm to 400 µm—at a laser scanning speed of 300 mm/s. The fluence used to texture the samples was between 13.4 Jcm^{-2} and 52.5 Jcm^{-2}. After processing, samples were cleaned with compressed air. The generated surface structures were imaged using a surface profilometer (Sensofar S mart) offering confocal, focus variation and interferometry measurement techniques in one system.

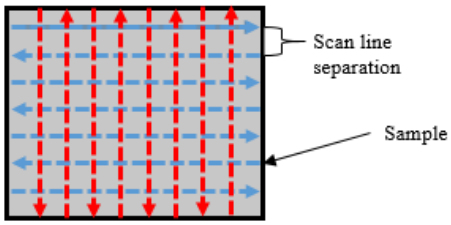

Figure 1: Schematic of laser scanning strategy employed to texture the stainless steel coupons.

The wettability of the processed surface textures was characterized using a contact angle meter (Attension Theta Lite), which can measure the static contact angle (θ_s) of deionized water droplets (~15 µL). Water droplets were released from the needle at a sufficient height that would avoid contact with the surface before release; using this method droplets rest freely on the surface without the influence of the needle. The dynamic behavior was assessed qualitatively by gently tilting the sample until (or if) the droplet rolled off.

Most of the samples were processed in air, however others were processed under argon (commonly used as a shielding gas in other laser processing applications), in order to prevent oxidation and hence examine the impact of oxidation on the result hydrophobicity. A laser processing chamber fabricated and used for the argon atmosphere processing. A schematic of this is shown in Figure 2.

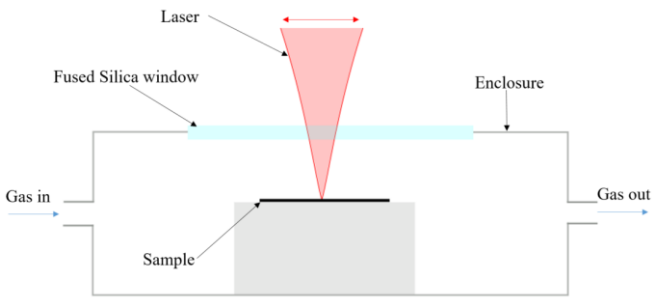

Figure 2: Schematic of the bespoke chamber used to process samples under a controlled environment.

3. RESULTS & DISCUSSION

3.1 Impact of fluence

Microstructures generated on SS304S15 with different fluences and a scan line separation of 100 µm, processed in air, are shown in Figure 3(A-C). The first pass with the laser creates a groove ~25-50 µm wide, whilst the second pass generates another groove perpendicular to the first with similar characteristics.

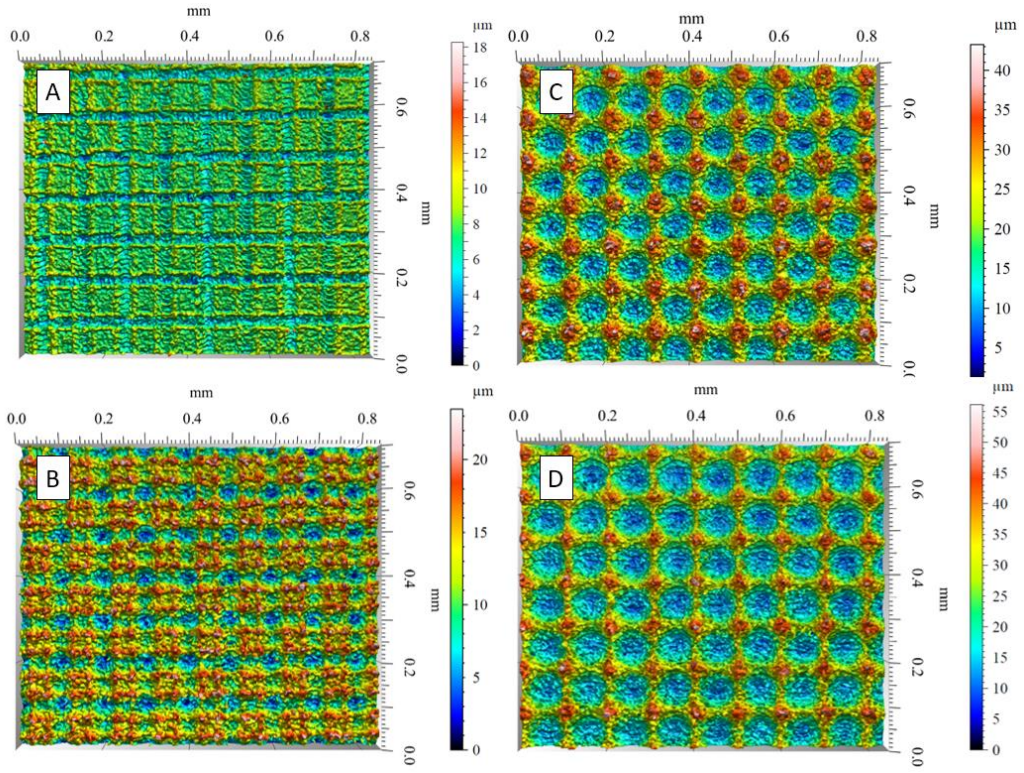

Figure 3: Microstructures generated with a scan line separation of 100 µm and laser fluence of (A) 13.4 Jcm^{-2}, (B) 20.1 Jcm^{-2}, (C) 45.1 Jcm^{-2} and (D) 52.5 Jcm^{-2} imaged using focus variation.

As expected, the width of the groove varies with laser fluence, with more material removed as the fluence increases, generating a wider groove. The resulting microstructure is one of micropillars of varying width and height. These micropillars are composed of part of the substrate which has not been directly irradiated, together with the material ejected as a result of laser processing. This ejected material then solidifies around the edges of the grooves, generating a structure in which its height is above the base material. The measured peak-to-trough height of these structures is displayed in Figure 4. It can be seen that there is a roughly linear relationship between laser fluence and peak-to-trough height, due to a combination of deeper grooves and more ejected material deposited at the edges of these grooves.

The anti-wetting transition (change in contact angle) for these microstructures is plotted in Figure 5. The structures are initially hydrophilic, but the contact angle increases with time, with some of them turning superhydrophobic eventually. For those samples processed with 52.5 Jcm^{-2} laser fluence, this transition has still not occurred after 50 days, reaching a maximum contact angle of ~100°. Meanwhile, samples processed with a laser fluence of either 35.4 Jcm^{-2} or 45.1 Jcm^{-2} both follow a similar evolution of contact angle, taking up to 50 days to achieve super hydrophobicity. However, samples processed with a laser fluence of 13.4 Jcm^{-2} show a sharp increase in contact angle after the first week, but further increases are minimal. Also, whilst a surface processed with 13.4 Jcm^{-2} reached a contact angle of 140°, the droplet did not slide away after gently tilting the sample, as required with a superhydrophobic surface. The microstructure with the shortest anti-wetting transition was that processed with a laser fluence of 20.1 Jcm^{-2}, reaching a superhydrophobic state after 2 weeks.

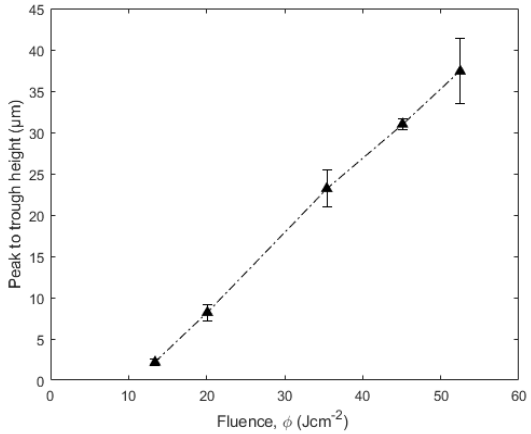

Figure 4: Peak-to-trough height as a function of applied fluence.

These results show that for structures textured with a scan line separation of 100 μm and laser fluence in the range 20.12 Jcm^{-2} to 52.5 Jcm^{-2}, the antiwetting transition time increases with applied fluence. Laser processing of stainless steel in air with nanosecond pulses will generate iron oxides. As observed in Figure 3, as the fluence is increased, a larger area of the surface is affected by the laser beam and so therefore it can be assumed that more iron oxide per unit area will be generated. These oxides are hydrophilic[10], and it is only after some time that the structures turn hydrophobic (or superhydrophobic). This indicates that there is a maximum rate at which the surface chemistry will change to being hydrophobic.

On the other hand, reducing the fluence to the point that a structure is barely apparent, such as those processed with a laser fluence of 13.4 Jcm^{-2}, initially yields a high contact angle, however this structure does not display a superhydrophobic state, indicating that a larger fluence is required for a final superhydrophobic state to be achieved. This suggests that either the surface chemistry is not favorable, due to an insufficient amount of oxide per unit area, or that the surface structure is not adequate for the generation of superhydrophobic structures.

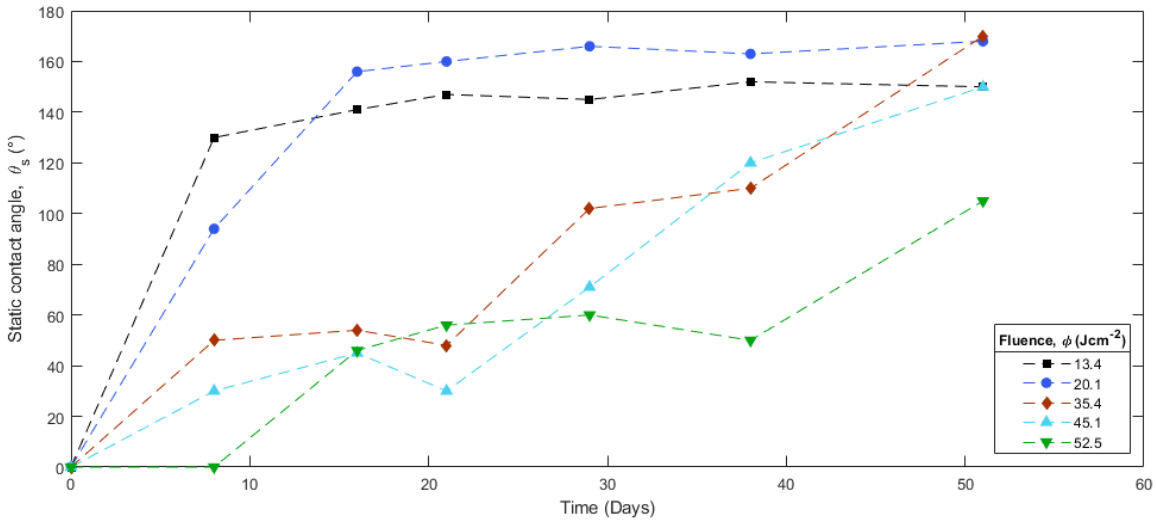

Figure 5: Anti-wetting transition of microstructures generated with 5 different laser fluences. The connecting lines are included as a guide to the eye and do not represent data or any kind of theoretical fit.

3.2 Impact of scan line separation

Structures generated with varying scan line separation and fluence were generated on SS304(SS15) as shown in Figure 6. For those structures processed with a scan line separation of 25 µm, it is not possible to obtain the same distinctive and repeating structure as that displayed in those scanned with 100 µm (Figure 3) and 200 µm (Figure 6) line separations. Instead a higher frequency roughness is the predominant texture. This is because the scan line separation is comparable with the beam size (~50 µm) and the generated grooves, with approximate widths of 35 µm and 60 µm for those processed with 13.4 Jcm^{-2} and 52.5 Jcm^{-2} laser fluences respectively.

For the textures generated with a scan line separation of 25 µm and 13.4 Jcm^{-2} observed in Figure 6 (A), (C), the highest regions of the texture appear to have a somewhat curved shape. These are similar to textures observed in the actual grooves of surface structures generated with the same fluence but a larger scan line separation, such as those displayed in Figure 6 (E). On the other hand, those processed with 52.5 Jcm^{-2} laser fluence display a structure in which the roughness and geometry is somewhat random.

As expected, as the scan line separation increases, so does the width of the remaining micropillars, e.g. comparing the structures displayed in Figure 3(A) and Figure 6(E). The structures generated with a 52.5 Jcm^{-2} laser fluence and a scan line separation of 100 µm and 200 µm observed in Figure 3(E) and Figure 6(F) respectively, where it can be seen that increasing the scan line significantly changes the texture.

The maximum measured contact angle for structures with varying fluence and scan line separations are plotted in Figure 7. Samples processed with 13.4 Jcm^{-2} are only superhydrophobic when generated with a scan line separation of 25 µm. For samples processed with a laser fluence of 20.1 Jcm^{-2}, all structures appeared to be superhydrophobic other than those processed with a scan line separation of 400 µm, which even though not superhydrophobic, displayed a contact angle of 150°. All samples processed with a laser fluence of 35.4 Jcm^{-2} achieved a superhydrophobic state, for the scan line separations tested in this work.

The anti-wetting results for surfaces processed from 100 µm to 400 µm scan line separation are somewhat expected, considering that other than the increasing spacing between the grooves; the general shape of the structures is similar. However, the fact that the structure processed with 20.1 Jcm^{-2} laser fluence and a scan line separation of 400 µm did not achieve a superhydrophobic state suggests that in this case the spacing between the peaks is too large, as those processed with higher fluence and therefore higher peak-to-trough distance did display superhydrophobicity.

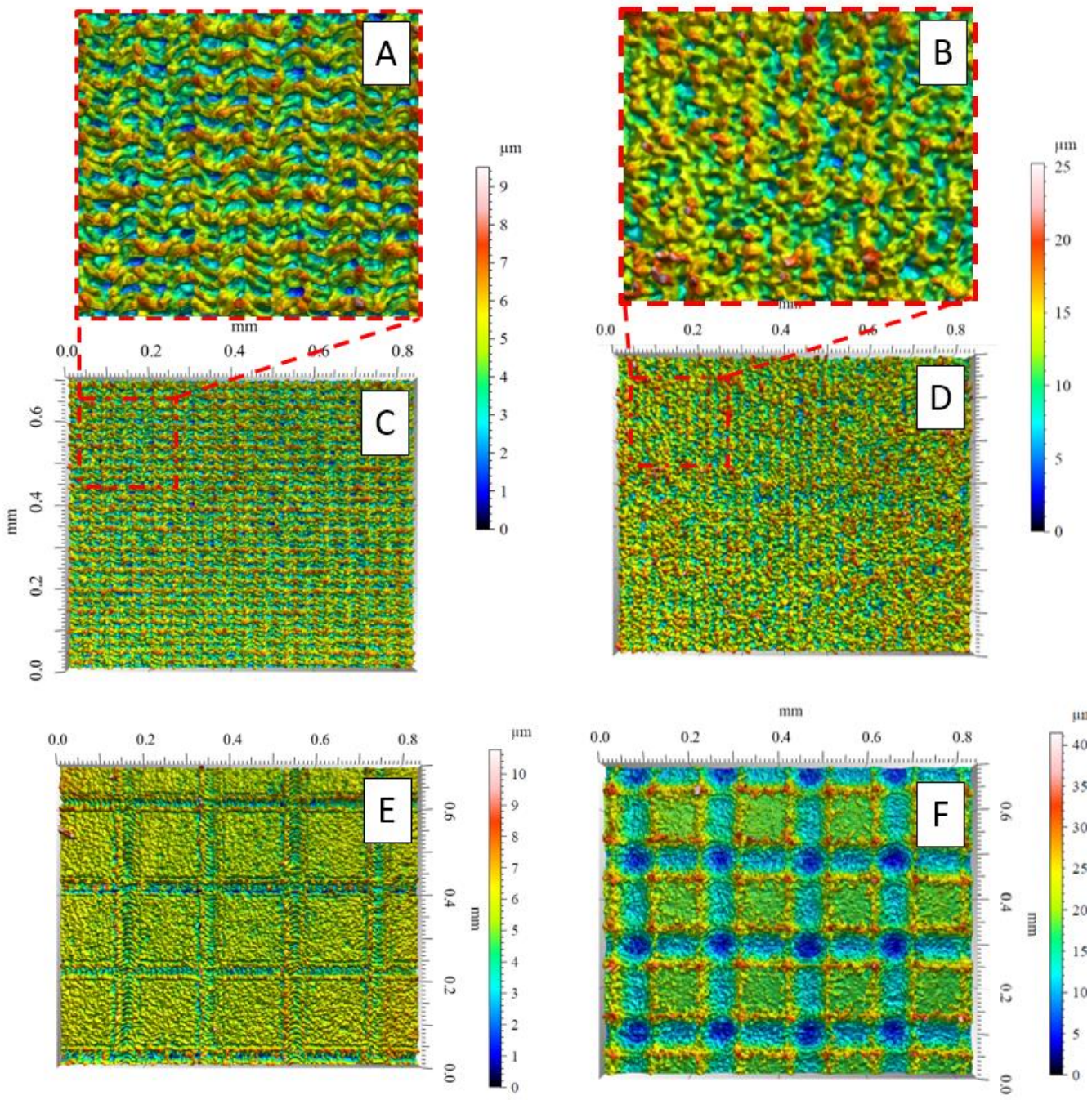

Figure 6: Surface structures generated with a scan line separation of 25 µm (A)-(D) and 200 µm (E)-(F). (A), (C), and (E) have been textured with 13.4 Jcm^{-2}, whilst (B), (D), (E) have been irradiated with 52.5 Jcm^{-2}.

Samples processed with 52.5 Jcm^{-2} and 45.1 Jcm^{-2} laser fluence displayed superhydrophobic behavior in all cases apart from those processed using a 25 µm scan line separation. As mentioned earlier, these structures have a higher frequency roughness somewhat similar to those processed with lower laser fluences, however those processed with lower laser fluences are superhydrophobic. This suggests that these structures may not have transitioned to a superhydrophobic state due to an unfavorable surface chemistry as a result of the laser texturing strategy—and therefore higher accumulated fluence.

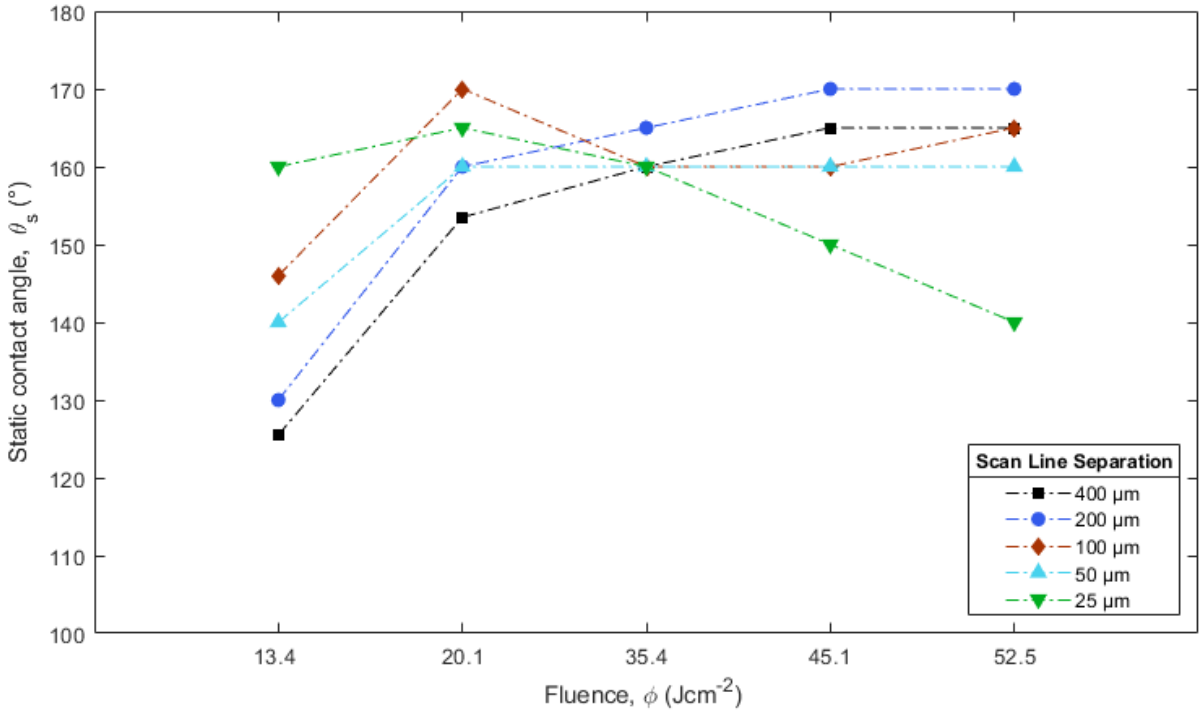

Figure 7: Static contact angle values of droplets for structures generated with varying scan line separation and fluence. The connecting lines are included as a guide to the eye and do not represent data or any kind of theoretical fit.

3.3 Processing environment: comparison between argon and air

The structures generated under an argon atmosphere appear grey instead of brown to the naked eye, indicating that oxidation has mostly been prevented in this case. The measured peak-to-trough height for textures generated under both argon and air are plotted in Figure 8 (A), both with a scan line separation of 100 µm for this work. In both cases, the peak-to-trough height increases as fluence is increased, however in argon these values are always smaller; presumably processing in air, extra energy is contributed from the exothermic oxidation reaction [13].

The impact of laser fluence on the anti-wetting transition for samples processed under argon is shown in Figure 8 (B). All samples developed a static contact angle of at least 100° in less than a week of storage. Structures generated with laser fluences of 35.4 Jcm^{-2}, 45.1 Jcm^{-2} and 52.5 Jcm^{-2} then transitioned to a superhydrophobic state three days later. This transition time is a significant improvement over those processed in air (Figure 5), and in these results appear not to be dependent on laser fluence, provided it is in this range. This suggests that whilst the amount of metal oxide in the surface has been minimized there is still sufficient for the anti-wetting transition mechanisms—described in Section 1—to take place. On the other hand, as mentioned earlier, this transition time has significantly shortened, indicating that a thinner surface metal oxide will accelerate the anti-wetting transition.

However, for samples processed using the lower laser fluence of 20.1 Jcm^{-2} the argon environment is detrimental to the anti-wetting transition since these structures never progressed into the same superhydrophobic state. Instead, the maximum contact angle measured was 100°, much lower than those processed in air, which transition into a superhydrophobic state after 2 weeks. When comparing them to structures of similar peak-to-trough height values, such as those processed with a scan line separation of 100 µm and a laser fluence 13.4 Jcm^{-2}, the latter whilst also not achieving a superhydrophobic state, do display a much larger static contact angle (150°). This suggests that there is insufficient metal oxide present in the structures, for either of the anti-wetting transition mechanisms to occur.

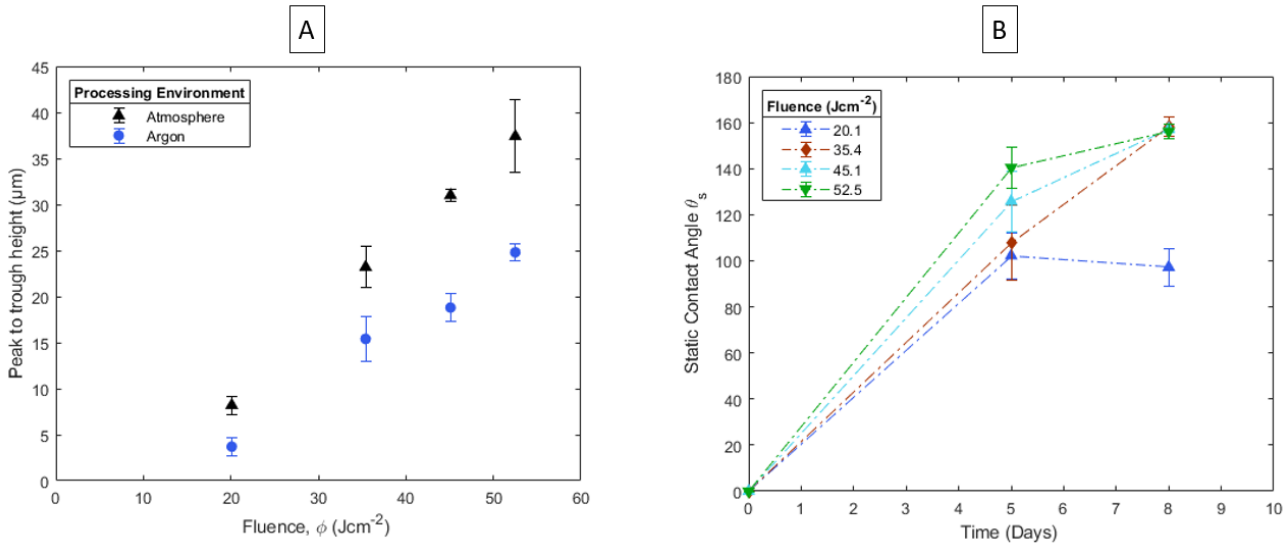

Figure 8: Peak-to-trough height of structures processed with a scan line separation of 100 µm (A), irradiated with laser fluences from 20.1 Jcm^{-2} to 52.5 Jcm^{-2} and different processing environments (Air and Argon). Anti-wetting transition of structures processed under an argon atmosphere (B).

4. CONCLUSION

Nanosecond pulsed lasers can be used to generate superhydrophobic surfaces using a simple raster scanning strategy, at 0° and 90°, to generate "checkerboard" type structures, provided that a correct combination of parameters are used. As with other laser-generation of superhydrophobic surfaces, there is a transition time required following laser processing in order for the surface to become hydrophobic. In this paper we have demonstrated that this transition time is strongly dependent on the laser processing parameters used. The degree of hydrophobicity that can be achieved is also directly affected by the atmosphere in which the processing is carried out.

Nanosecond lasers are also suitable for generating superhydrophobic structures, for structures processed with a scan line separation of 100 µm and laser fluence from 20.1 Jcm^{-2} to 52.5 Jcm^{-2}. The anti-wetting transition time increases as the laser fluence is increased, however texturing with this same scan line separation and 13.4 Jcm^{-2} is not suitable for the generation of anti-wetting structures. Increasing the scan line separation from 50 µm to 300 µm, will yield similar results in terms of superhydrophobicity for laser fluences from 20.1 Jcm^{-2} to 52.5 Jcm^{-2}. Increasing the scan line separation beyond this point, will result in structures that are not superhydrophobic if textured with 20.1 Jcm^{-2} laser fluence. On the other hand, decreasing the scan line separation to 25 µm allows lower laser fluences (13.4 Jcm^{-2}) to generate superhydrophobic structures.

Laser texturing SS405(S15) under an argon atmosphere will yield similar structures to those generated with air when using a scan line separation of 100 µm and laser fluences 20.1 Jcm^{-2} to 52.5 Jcm^{-2}. However due to a lower removal rate, the structures textured in an under an argon atmosphere will have a smaller peak to trough height compared to those processed in air. In some cases, processing under an argon atmosphere will yield textures that transition to a superhydrophobic state several times faster than those processed under an air atmosphere.

ACKNOWLEDGMENTS

This research was supported by the EPSRC through the Centre for Doctoral Training in Applied Photonics and from the European Union's Horizon 2020 research and innovation programme under grant agreement No 768701.

5. REFERENCES

[1] Kulinich, S. A., Farhadi, S., Nose, K. and Du, X. W., "Superhydrophobic surfaces: Are they really ice-repellent?," Langmuir **27**(1), 25–29 (2011).

[2] Fürstner, R., Barthlott, W., Neinhuis, C. and Walzel, P., "Wetting and self-cleaning properties of artificial superhydrophobic surfaces," Langmuir **21**(3), 956–961 (2005).

[3] Barthlott, W. and Neinhuis, C., "Purity of the sacred lotus, or escape from contamination in biological surfaces," Planta **202**(1), 1–8 (1997).

[4] Vorobyev, A. Y. and Guo, C., "Direct femtosecond laser surface nano / microstructuring and its applications," 1–23 (2012).

[5] Ta, V. D., Dunn, A., Wasley, T. J., Li, J., Kay, R. W., Stringer, J., Smith, P. J., Esenturk, E., Connaughton, C. and Shephard, J. D., "Laser textured superhydrophobic surfaces and their applications for homogeneous spot deposition," 153–159 (2016).

[6] Jagdheesh, R., García-Ballesteros, J. J. and Ocaña, J. L., "One-step fabrication of near superhydrophobic aluminum surface by nanosecond laser ablation," Appl. Surf. Sci. **374**, 2–11 (2016).

[7] Ta, D. V, Dunn, A., Wasley, T. J., Kay, R. W., Stringer, J., Smith, P. J., Connaughton, C. and Shephard, J. D., "Nanosecond laser textured superhydrophobic metallic surfaces and their chemical sensing applications," 248–254 (2015).

[8] Ngo, C. V. and Chun, D. M., "Fast wettability transition from hydrophilic to superhydrophobic laser-textured stainless steel surfaces under low-temperature annealing," Appl. Surf. Sci. **409**, 232–240 (2017).

[9] Cardoso, J. T., Garcia-Girón, A., Romano, J. M., Huerta-Murillo, D., Jagdheesh, R., Walker, M., Dimov, S. S. and Ocaña, J. L., "Influence of ambient conditions on the evolution of wettability properties of an IR-, ns-laser textured aluminium alloy," RSC Adv. **7**(63), 39617–39627 (2017).

[10] Jagdheesh, R., Diaz, M., Marimuthu, S. and Ocana, J. L., "Robust fabrication of μ-patterns with tunable and durable wetting properties: hydrophilic to ultrahydrophobic via a vacuum process," J. Mater. Chem. A **5**(15), 7125–7136 (2017).

[11] Kietzig, A. M., Hatzikiriakos, S. G. and Englezos, P., "Patterned superhydrophobic metallic surfaces," Langmuir **25**(8), 4821–4827 (2009).

[12] Chun, D. M., Ngo, C. V. and Lee, K. M., "Fast fabrication of superhydrophobic metallic surface using nanosecond laser texturing and low-temperature annealing," CIRP Ann. - Manuf. Technol. **65**(1), 519–522 (2016).

[13] Ghany, K. A., Newishy, M., "Cutting of 1.2mm thick austenitic stainless steel sheet using pulsed and CW Nd:YAG laser," Journal of Materials Processing Technology **168**(3), 438–447 (2005).